# Detectors of Cosmic Rays, Gamma Rays, and Neutrinos

A. Altamirano*,† and G. Navarra**

*Departamento de Física, Informática y Matemáticas, Facultad de Ciencias y Filosofia, Universidad Peruana Cayetano Heredia
†Centro de Tecnologías de Información y Comunicaciones (CTIC), Universidad Nacional de Ingeniería, Lima, Perú
**Dipartimento di Fisica Generale dell'Universita' and INFN, Torino, Italy

**Abstract.** We summarize the main features, properties and performances of the typical detectors in use in Cosmic Ray Physics. A brief historical and general introduction will focus on the main classes and requirements of such detectors.

**Keywords:** Detectors; Cosmic Rays; Gamma Rays; Neutrinos
**PACS:** 96.50.S-; 95.55.Ka; 98.70.Sa; 29.40.-n

## INTRODUCTION

As for all experimental Sciences, the development of knowledge in Cosmic Ray Physics has been, and is, strongly connected with the development of instrumentation and therefore of radiation detectors. As a general introduction, we want to outline here the peculiarities and ranges covered by cosmic ray detectors, that are characterized by quite different requirements.

- Concerning the energies of interest[1], neutrinos cover the domain from MeV (solar and supernova) to EeV (cosmogenic), gamma rays from keV to TeV (diffuse, bursts, sources), with the additional interest for the possible diffuse flux at EeV energies (cosmogenic, or due to "non standard astrophysical acceleration processes", as from the so-called Top-Down models), while charged cosmic ray particles are studied from MeV to ZeV energies (see e.g. refs [1, 2, 3]).

- From the point of view of the "location", from the comparison of the depth of the atmosphere ($X \approx 1000$ g/cm$^2$) with the typical interaction lengths of the incoming particles ($X_0 \approx 37.7$ g/cm$^2$ for e.m. primaries, $\lambda \approx 90$ g/cm$^2$ for protons), we deduce that, if we require that the incoming particle interacts inside the detector (what we call *direct* experiments), we need to operate at altitudes above 15 km, i.e. with satellite or

[1] About energy notations: keV=$10^3$ eV; MeV=$10^6$ eV; GeV=$10^9$ eV; TeV= $10^{12}$ eV; PeV= $10^{15}$ eV; EeV= $10^{18}$ eV; ZeV= $10^{21}$ eV. Depths in an absorber are usually measured in units of $x = l \cdot \rho$ i.e. *length* x *density*, with dimensions: [cm] $\cdot$ [g/cm$^3$] = [g/cm$^2$].

CP1123, *Cosmic Rays and Astrophysics*, edited by C. J. Solano Salinas, D. Wahl, J. Bellido, and Ó. Saavedra

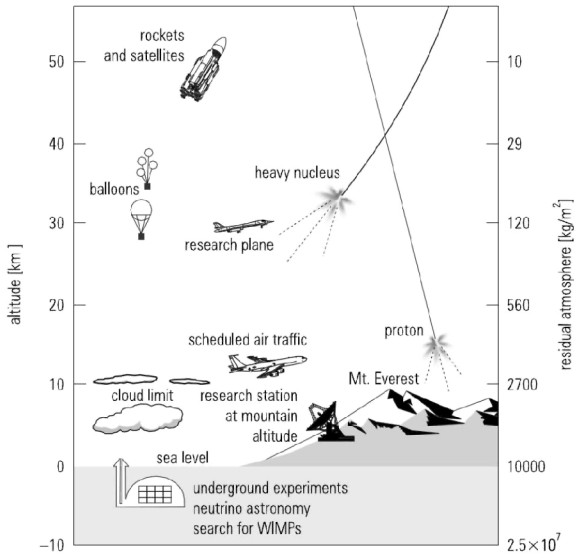


**FIGURE 1.** An atmospheric profile showing the typical primary interactions altitudes.

balloon born detectors (see Fig.1) [2]. Such equipments, being limited in dimensions and weight, are obviously limited at high primary energies, due to the low fluxes (that impose large sensitive areas) and the weight required for the instrumentation. Typically, for charged particles, this occurs at about $10^{14}$ - $10^{15}$ eV, where the primary flux goes below 1 particle per square meter per month. At sufficiently high energies, the cascades induced by the primary interactions in the atmosphere (as well as the secondaries produced underground by neutrinos) can be detected at ground and mountain levels (or underground/underwater for neutrinos), with the so called *indirect* experiments. The relation between the primary spectrum and the required effective areas of the detectors can be deduced from Fig. 2.

- This introduces the theme of the dimensions and running times of the installations. As we can see from Fig.2, at the highest energies, detectors of huge dimensions are required (the larger acceptance running array, the Auger Observatory, has an effective acceptance area of 3000 $km^2$), and this has to be coupled to long observation times (of the order of 20 years). Such requirement does not only apply to the highest energies, but to lower energies as well, when effects of small amplitude have to be studied (see e.g. the case of anisotropies in which the amplitudes, and therefore the required sensitivities are of the order of $10^{-4}$ - $10^{-3}$). And of course this rises the requirement for long time stabilities (and therefore monitoring and maintenance) of the operators, for arrays usually located in peculiar sites (always for the case of the Auger Observatory, the argentinean pampa), and very far from "laboratory" conditions.

From historical point of view [4, 5, 6], we will just list here the main steps that have accompanied the growth of cosmic ray physics: from the traditional and the Wulf

[2] The situation is different for neutrinos, for which the interaction length ($\lambda \approx 10^{13}$ g/cm$^2$) requires extremely large detector dimensions, shielded against the charged cosmic ray induced background.

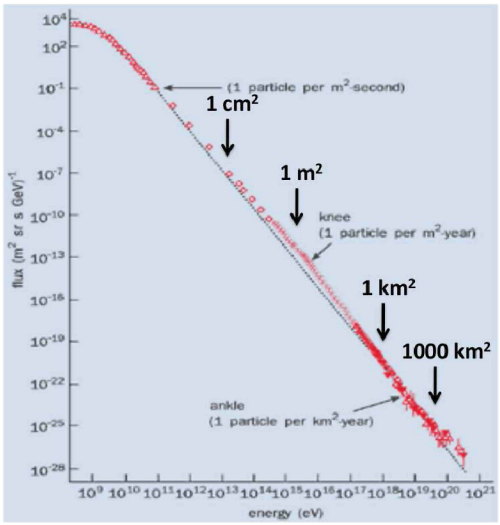


**FIGURE 2.** Cosmic ray primary intensity: the typical detector dimensions necessary to observe one event/month are given.

electroscopes that marked their discovery (V.F. Hess, 1912), to the time resolving single particle detectors (Geiger counters) and electronic circuits (Rossi coincidence), that allowed, beside basic experiments [3], the growth of modern (correlated) arrays and methods. Tracking and high resolution techniques (as cloud chambers, nuclear emulsions) represent examples of other families of detectors that have marked the development of cosmic ray and particle physics, that for long time have been (and still are) interconnected. On another side the development of scintillators[4], and of Cherenkov light detectors[5] have provided new tools both for precision measurements and for practicable large area and volume sensitive devices. The basic physics processes are the ones exploited in nuclear and high energy physics [7, 8].

Among the technical developments that have made possible significant achievements we have to remind the space technology, that provided the opportunity of high sensitivity measurements in direct experiments (on balloons and satellites, and among them the recent long duration flights realized in Antarctica[9]), and the high speed and communication techniques that made possible the quoted large dimension arrays as the Auger Observatory.

---

[3] We remind the proof by Bothe and Kohlhoster (1929) of the charged nature of cosmic ray secondaries.

[4] The energy losses of charged particles (see (1)) produce excitation of the material, and therefore, when de-excitation occurs, a detectable scintillation light. Assuming, as typical amount of energy required for producing a detectable photon, $E_\gamma \approx 100$ eV, the number of produced photons is $N_{ph} \approx 2 \cdot 10^4$ ph /g/cm$^2$.

[5] We remind the number of emitted Cherenkov photons: $d^2N_{ph}/dxd\lambda = (2\pi Z^2\alpha/\lambda^2) \cdot sin^2\theta_c$, where $sin^2\theta_c = (1 - 1/(\beta^2 n^2))$; $\alpha = 1/137$, Z is the particle charge in electron charge units, $\beta$ the particle velocity relative to the speed of light, $n$ the refractive index of the medium. The detector is therefore sensitive to the particle velocity, and is characterized by a threshold: $\beta > 1/n$. The limit angle for ultra-relativistic particles is $\theta = 1/n$.

As an interesting feature, we want to stress here the complementarity of the detectors with the space environment. In fact we want to study the particles coming from the external space, also to obtain information on their propagation in space; but the "space" itself may constitute part of the detector. The first understanding of primary radiation (charged vs neutral, and the identification of the predominant charge) required a magnetic analyzer, and for that the Earth magnetic field was exploited and played a fundamental role (as pioneers of such works: J. Clay, A.H. Compton, T.H Johnson, L.W. Alvarez, and B. Rossi). This was recently exploited in satellite experiments as an isotope analyzer[10], and we expect the method to be extended to the highest energies through the Milky Way magnetic field.

## COSMIC RAYS: SPACE DETECTORS

### *Basic detector*

The interaction inside the detector allows very accurate studies of the primary, from the points of view of energy measurement and particle identification. From the basic properties of the e.m. interactions of charged particles we obtain, as typical energy losses($\beta$ is the particle velocity, Z its charge; the correct expression is Bethe-Bloch[11]):

$$-\frac{dE_0}{dx} \approx 2 \cdot \frac{Z^2}{\beta^2} \cdot log(f(Ip,\beta)) \frac{MeV}{gr \cdot cm^{-2}} \tag{1}$$

This, together with a typical detector scheme, is shown in Fig. 3. It is easy to verify that from combined measurements of the kinetic energy ($E_o$) and of the energy loss in a thin detector (e.g. a scintillator), the charge (atomic number) can be deduced. At non-relativistic energies, the relation: $1/\beta^2 \propto M/Eo$ leads additionally to the possibility of identifying the particle mass (isotopic nucleus)[12].

If the particle energy is large enough (above critical energy to radiate or above $\pi^o$ production threshold) electromagnetic cascades are produced. Examples of cascade curves in atmosphere are given in Fig. 4: they are ruled by subsequent processes of electron bremmstrahlung and photon pair production. E.m. cascades develop in quite similar way in all media, if the cascade description is performed in terms of radiation length ($X_o$) for the depth in the material, and critical energy $E_c$ for energy scale. The e.m. cascade develops till the average energy is larger than $E_c$ (i.e. radiation processes dominate), than the energy losses by collision dominate and the cascade is absorbed. Since finally all energy is dissipated through collision energy losses, it is converted into a measurable signal (e.g. photons, or other quanta detectable by a sensitive device) inside the detector (principle of calorimetric energy measurements).

All quoted effects depend on the charge as "$Z^2$"; mainly the search for anti-matter requires "Z" sensitive detectors, as typically provided by magnetic deflections, and

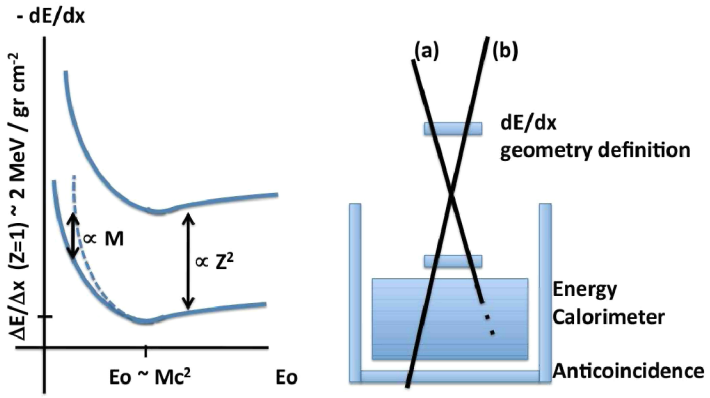


**FIGURE 3.** Schematics of energy losses and of particle identification and energy measurement in space experiments (the role of the anticoincidence is to guarantee full containment of the energy released by the incident nucleus, i.e. separating trajectories (a) and (b)).

on such principle main space detectors are now operating. This further provides an additional energy measurement[13, 14]. Direct Measurements of Cosmic Rays are discussed in these proceedings (see ref [15]), references to specific NASA missions and detectors can be found in[16].

## *Principles of calorimetry*

Given $Eq$ as the energy required to produce a detectable "quantum" inside the calorimeter (a photon for a scintillator, a pair for a semiconductor device, an electron-ion for a gas array, etc.), the number of produced quanta is $No = Eo/Eq$, and $N = \varepsilon \cdot No$ is the actual number of recorded quanta ($\varepsilon$ being the collection and detection efficiency of the sensitive element[6]) the resolution is $\frac{\sigma(Eo)}{Eo} = \frac{\sigma(N)}{N} = \frac{\sqrt{N}}{N} = \frac{1}{\sqrt{N}} = \sqrt{\frac{Eq}{\varepsilon \cdot Eo}}$ (i.e. dominated by poisson fluctuations, that represent the physical limitation). The resolution improves with increasing primary energy, and is better for smaller values of $\sqrt{\frac{Eq}{\varepsilon}}$, i.e. better for detectors based on physical principles with smaller values of $Eq$ (better semiconductor devices, for which $Eq \approx 1$ eV, than scintillators, for which $Eq \approx 100$ eV). Typical resolutions are or the order of $\frac{\sigma(Eo)}{Eo} \approx \frac{10\%}{\sqrt{Eo[MeV]}}$[17, 18].

---

[6] It is easy to show, by following a recursive procedure, that, for wide ranges of detectors' dimensions: $\varepsilon = q_e \cdot e/(1-x)$, where $e = S_{sd}/(2\pi d^2)$, $x = r_w(1-e)exp(-d/\lambda_a)$, $S_{sd}$= surface of sensitive device, $d$ = detector linear dimension, $r_w$ = reflectivity of the walls, $\lambda_a$ = attenuation length of the signal inside the detector material, $q_e$ = quantum efficiency of the sensitive element.

### *Sampling calorimeters*

For high primary energies, a large amount of energy is released in an e.m. cascade, and this may be difficult to be contained inside the sensitive volume. A significant improvement has been obtained by using alternated layers of sensitive material and absorbers (characterized by a small radiation length). Based on such principle, the primary spectrum has been studied up to about $10^{15}$ eV by means of the Proton series satellites already in 1960's[19]. More recently it has been exploited in balloon born and in ground based experiments. The energy resolution is more difficult to be evaluated, depending on more parameters; it was about 20% for the Proton case at about 30 GeV.

### *Single interaction measurements*

In nuclear emulsions the classical energy measurements were based on the kinematics of secondary particle production deduced from their emission angles[20]. The method has been extended to higher energies by studying the angle and energy of the e.m. cascades from the decays of the $\pi^0$ produced in the first interaction of the primary in the detector[21, 22]. By using stacks of emulsion (or X-rays) chambers, good accurcies are obtained in the measurement of the energy released in the e.m. component in such interaction (about 15%); more complex (due to intrinsic fluctuations) is the conversion from the energy loss in a single act to the total energy. Electronic detectors based on semiconductor sensitive elements have recently been developed, and applied to long duration flights[23, 24].

## GAMMA RAYS: SPACE DETECTORS

The basic physical principles can be naturally extended to primary gamma rays. Gamma rays do not produce directly ionization, but they produce electrons in the detectors through photoelectric effect, Compton scattering, and $e^+e^-$ pair production. At high energies the latter is the dominating process, and therefore the calorimetric measurement of the cascade provides the natural energy estimator. Gamma rays are not deflected by the galactic magnetic fields and therefore bring the direct information on their source. Arrival direction measurements are performed through the $e^+e^-$ directions in a tracking detector (gas chamber, semiconductor device...). The arrival direction accuracy is better or of the order of $1^o$ in the GeV energy region. Due to the fluxes, and the thickness limitations, the method is effective up to energies of the order of 10 GeV (GLAST will go beyond 100 GeV). As an additional requirement, being the gamma ray flux much lower than the charged cosmic ray one, an anticoincidence has to be operated around the whole installation in order to identify the signals from charged cosmic ray particles. As references see e.g. [25, 26, 27].

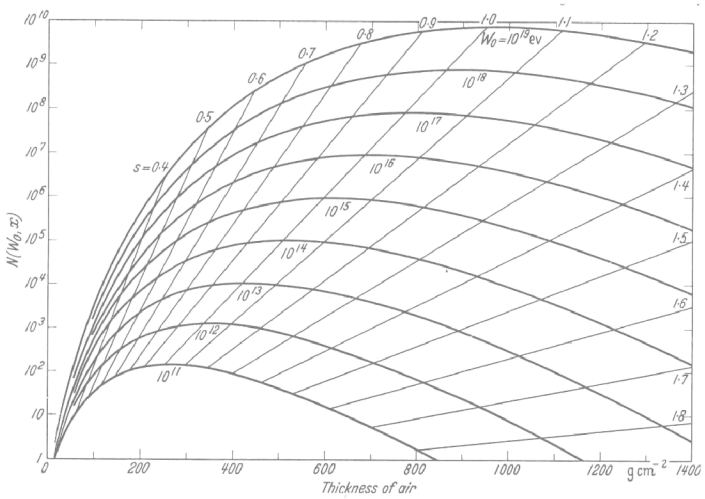


**FIGURE 4.** Longitudinal developments of e.m. cascades in atmosphere. Conversion to other absorbers ($a$) can be performed by converting the thickness $t$ to $t_a = t \cdot X_0^a/37.7$ g·cm$^{-2}$, and the energy $E$ given above the curves to $E_a = E \cdot E_c^a/81$ MeV, where $X_0$ is the radiation length and $E_c$ is the critical energy.

# COSMIC RAYS: GROUND BASED DETECTORS

## *Surface arrays*

As we can deduce from Fig. 2, above $10^{15}$ eV the dimensions of space detectors (besides the increasing limitations in energy determination) do not allow the use of such methods to extend the study of the spectrum. The development of ground based arrays (see Fig. 5) is therefore compulsory. At such high energies the interactions of primary nuclei are characterized by multiple secondary production (pions, kaons...). Among such secondaries $\pi^o$s decay into gammas while $\pi^{+/-}$ may interact or decay into muons and neutrinos. A cascade (Extensive Air Shower, EAS[28]) is produced, dominated by the e.m. secondaries. From Fig. 4 it is possible to check that a $10^{15}$ eV e.m. cascade reaches its maximum development at a depth of about 600 g·cm$^{-2}$ (i.e. about 4000 m a.s.l.) and the number of particles is about $10^6$ (about $10^5$ at sea level). A main feature that allows the detection of EAS particles over large effective areas is related to their lateral distribution. In fact, due to the Coulomb scattering, the particles of the cascade are spread over large distances from the shower axis, the typical distance being $R_m = E_s/E_{crit} \cdot X_0$, with $E_s \approx 21$ MeV. $R_m$ (Moliere radius) is about 75 m at sea level. Assuming that all particles ($10^5$-$10^6$ in our example) are distributed over a surface of radius $R_m$ ($S \approx 10^4$m$^2$) we obtain an average density of a few particles per square meter, i.e. detectable with one square meter sensitive area, up to distances of the order of 100 m from the shower axis.

Such sampling technique provides the opportunity of realizing collecting areas much larger than the active ones. The sensitive/effective areas ratios range from $3 \cdot 10^{-3}$ for EAS-TOP (33 x 10 m$^2$ elements over $10^5$ m$^2$) to $5 \cdot 10^{-6}$ for the Auger surface detector

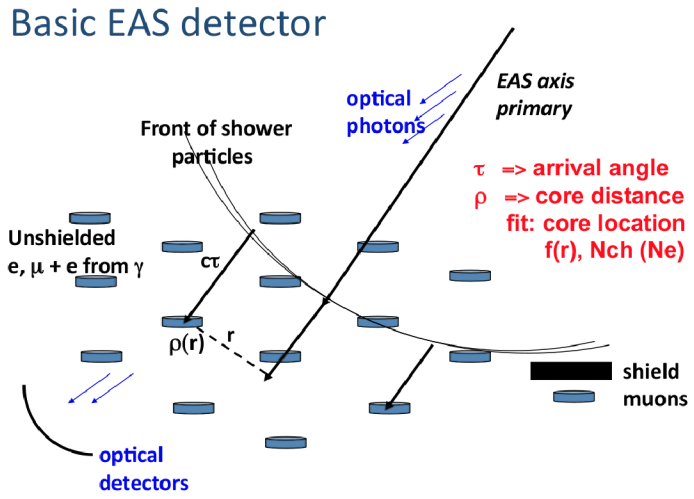


**FIGURE 5.** General scheme of an Extensive Air Shower detector.

(1600 x 10 $m^2$ elements over 3000 $km^2$). Among historical extensive air shower arrays we remind: for the intermediate energy region ($10^{15}$ - $10^{16}$ eV, relevant for the studies of the "knee" region)): Moscow State University[29], CASA-Mia, EAS-TOP[30], GRAPES[31], KASCADE[32] and KASCADE-Grande[32] (extending up to $10^{18}$ eV), IceTop[33] ; for the highest energy region (above $10^{18}$ eV): Volcano Ranch[34], Haverah Park[35], AGASA[36], Auger[37].

Among the air shower particles reaching the observation level we want to mention here the muon component, that has played a very important role in the studies of primary composition. Low energy muons (below GeV) mainly decay and do not reach the ground. Muons reaching the ground are therefore of higher energy with respect to electrons, and therefore are not significantly affected by the Coulomb scattering; they are spread on the ground mainly due to the transverse momentum ($p_t$) at their parent pion production (typically: $r \approx p_t \cdot h/E \approx 0.5[GeV] \cdot 2000[m]/5[GeV] = 200$ m, generally larger but similar to the e.m. spread). As a general property, while the e.m. cascades develop and are subsequently absorbed, the produced muon component is not significantly attenuated[7].

This provides a tool for primary composition studies: if we assume that a cascade produced by a nucleus of mass A is equivalent to the sum of A proton cascades, for

[7] We remember that the energy loss by radiation, being classically related to a charge acceleration in an electric field, is inversely proportional to the square of the mass of the particle. Therefore the radiation length which is 37.7 g/$cm^2$ for electrons becomes 1.6 $10^6$ g/$cm^2$ for muons, that therefore loose energy mainly by "collisions" (i.e. excitation and ionization). And this moreover provides a main technique for muon detection against the much higher e.m. background: a shielding of a sufficient thickness of radiation units of material (20 $X_0$ for KASCADE) can absorb the e.m. component without significantly affecting the muon one.

showers detected after their maximum, we have $N_e \propto A \cdot (Eo/A)^{\alpha}$ and $N_\mu \propto A \cdot (Eo/A)^{\beta}$, where $\alpha \approx 1.2$, and $\beta \approx 0.95$. And therefore, by eliminating $E_o$ (that is not measured, while $N_e$ and $N_\mu$, respectively the electron and muon numbers, are our observables), we obtain: $N_\mu \propto A^{1-\beta/\alpha} \cdot N_e^{\beta/\alpha}$, i.e., with the quoted values: $N_\mu \propto A^{0.2} \cdot N_e^{0.8}$ (i.e., for fixed electron number, the number of muons for primary iron nuclei is about a factor of 2 larger than for protons). The number of muons is much smaller that the electron one (from 1% to 10%, depending on the atmospheric depth).

An intrinsic issue, strictly related to the detector, is the reconstruction procedure. For sensitive units of thickness smaller than the radiation length, all charged particles loose the same amount of energy (the minimum ionizing particle, "m.i.p.", corresponding to the minimum of the curve of Fig. 3, and only logarithmically increasing with energy). From measurements of particle densities at different locations on the ground, the core location (xc, yc), and total number of particles ($N_{ch}$, essentially electrons and muons) are obtained by means of a fit to a theoretical (or phenomenological) expression of the charged particles' lateral distribution. The arrival direction is obtained from the arrival delays of particles at the different locations (easy to understand if we assume, as first approximation of the shower disc, a plane with negligible thickness; the fact that the shower disc is not a real plane and has a non negligible thickness introduces an uncertainty of the order of the degree).

In case that the sensitive units are thicker than the radiation length, electrons usually loose all their energy, photons convert into electrons, and therefore release all their energy as well, while muons cross the whole detector and release an amount of energy dependent on the detector thickness (e.g. 250 MeV for the Auger tanks of thickness 1.2 m). The reconstruction procedure is basically similar, but what is reconstructed is a "signal" to which different particles contribute with different weights.

If the units' spacing is much larger than the Moliere radius, the total number of particles can be hardly determined with an acceptable uncertainty, and it may be convenient to derive the signal amplitude at a given core distance $R_{opt}$. Such distance depends on the detector configuration, and can be related to the primary energy ($R_{opt}$ ranges from 600 m for Haverah Park and Akeno, to 1000 m for the Auger array).

The individual elements of the array can be continuously calibrated by means of the high rate muon flux, that provides the response to the energy loss of a "minimum ionizing particle" (that is the basic measurement unit), keeping the fluctuations at the poissonian level. Combining this with the quoted reconstruction procedure, the obtained typical accuracies are about 10% both in $N_{ch}$ (KASCADE-Grande) and S(1000 m) (Auger).

The conversion to primary energy can be performed through different techniques (simulations, or phenomenological methods). But essentially all methods, both concerning energy measurements and primary composition studies, are subject to the uncertainties due to the shower to shower fluctuations. An idea of the extent of such fluctuations, obtained from simulations[38][8], is given in Fig. 6; obviously they affect all data obtained at "fixed atmospheric depth". A remarkable improvement can be obtained by observing the whole atmosphere (that in fact provides a real calorimetric information). The observation of the whole cascade development can be performed by exploiting the optical emission of the charged particles in the atmosphere (Cherenkov[9] or fluorescence[10] light). The total light intensity of the two signals is of the same order of magnitude. Cherenkov light is however concentrated inside an opening angle of about 1 degree, while fluorescence emission is isotropic. As a consequence, the ratio of the two, inside such angle, is of the order of $10^{-4}$ - $10^{-5}$. And this explains the different typical energies and applications of the two families of detectors (about $10^{12}$ eV for directional observations, and $10^{15}$ eV for wide angular aperture Cherenkov arrays; around $10^{17}$ - $10^{18}$ eV for fluorescence). Concerning calibrations, they have to be performed at the photoelectron level, that for individual PMTs can be realized at the 10% level accuracy.

The main source of uncertainty of the fluorescence technique is however still due to the uncertainty in the "fluorescence photon yield", i.e. the amount of energy loss converted into fluorescence emission. Such indetermination, together with its dependence on pressure and temperature amounts to about 15%. No "photon yield" systematic uncertainty affects Cherenkov light emission.

Such observations are obviously possible in clear, moonless nights (the corresponding duty cycle being of about 10%), and the related energy thresholds depend on the fluctuations of the night sky background in the respective wavelength ranges (see next section). We have moreover to remind that monitoring of atmospheric condition is a necessary, complementary tool for such observations[40], and that the related uncertainties introduce further limitations to the accuracies of the measurements.

But, in spite of such limitations, optical detectors, using the whole atmosphere as a "calorimeter" can provide energy measurements largely independent from calcula-

---

[8] We want to stress here, together with the development of detectors, the importance of simulations that allow to include their response inside realistic representations of the physical phenomena under study, providing meaningful comparisons with experimental data[39].

[9] The refractive index in atmosphere can be described as $n = 1 + \eta$, where $\eta = \eta_0 \cdot x/x_0$, $x$ = atmospheric depth, $x_0$ = atmospheric depth at sea level, $\eta_0 = 2.9 \cdot 10^{-4}$; the maximum emission angle is: $\theta \approx \sqrt{2\eta} \approx 7.5 \cdot 10^{-4}\sqrt{x}$, i.e. $1.3^o$ at sea level; the energy threshold is 21 MeV for electrons, and 4.3 GeV for muons. The number of photons emitted in the wavelength range $350 < \lambda < 500$ nm, by a $\beta \approx 1$ and Z=1 particle, is $dN/dl = 786 \cdot \eta$ ph/cm, i.e. at sea level 23 ph/m.

[10] Fluorescence emission in atmosphere is mainly due to Nitrogen excitation. The emitted light amounts to about 4.8 ph/m at sea level, concentrated in a few lines between 300 and 430 nm.

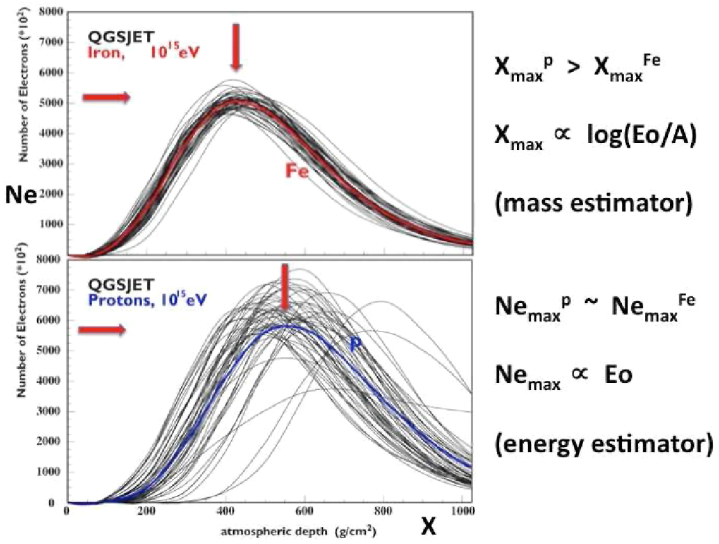


**FIGURE 6.** Simulated longitudinal profiles of cascades from different primaries. The extent of fluctuations is shown (smaller for heavy primaries, since the cascade from a nucleus of mass A can be considered to be built from the superposition of A proton showers, and therefore fluctuations are reduced of a factor approximately $\sqrt{A}$).

tions involving hadron interaction properties (which is of upmost importance at the highest energies). Such techniques provide, moreover, the measurement of the depth of maximum development of the cascade, that is related to the primary mass (see Fig. 6). This is usually obtained by the direct observation of the cascade curve by the fluorescence arrays, and by means of the conversion of the light lateral distribution into the longitudinal shower development, for the case of Cherenkov light arrays. Typical observation conditions of fluorescence and Cherenkov light in EAS are sketched in Fig. 7; for recent results related to the energy and depth of shower maximum measurements see refs [37, 41, 42, 43][11].

## GAMMA RAYS: GROUND BASED DETECTORS

Standard EAS arrays are sensitive to primary gamma rays through the detectors of the e.m. component[30, 44]. Different configurations have been and are exploited (as main methods to enhance the sensitivity to gamma primaries we remind: the detection of the muon component in EAS, the accurate study of the lateral distribution, high altitude and continuous arrays to reduce the primary energy to the energy region of interest)[45, 46].

We want however to focus here on the class of detectors that have mainly contributed, till now, to construct the knowledge of gamma ray sources and connect the information

[11] A full integration of the surface and optical techniques has recently been realized by the Auger Observatory[37].

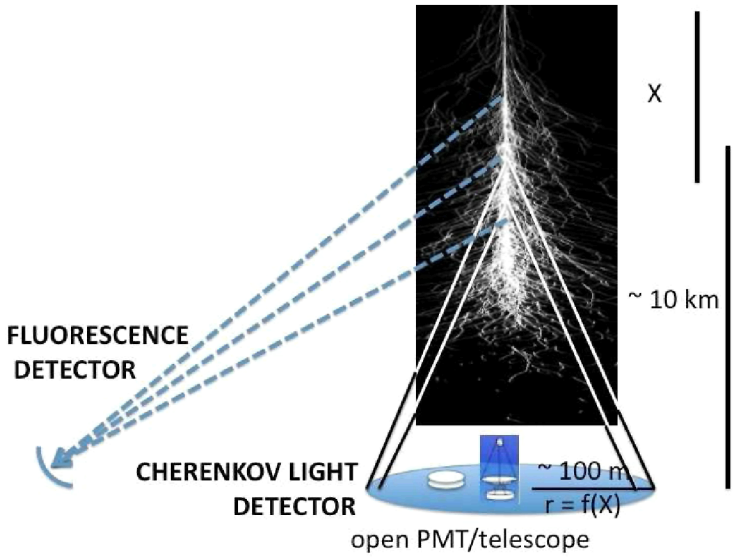


**FIGURE 7.** Scheme of optical detectors: fluorescence and Cherenkov radiations. Depending on primary energy Cherenkov light can be recorded by means of wide angle open arrays (large field of view, limited collecting area, $E_0 > 10^{15}$ eV), or telescopes (small field of view, large collecting area, $E_0 > 10^{11}$ eV).

with the satellite data. From the previous discussion about optical detectors, we observe that a "natural" effect pointing at the energy region of interest ($10^2$- $10^3$ GeV) and at large effective areas can be provided by the atmospheric Cherenkov light emission, since from a single observation point events distant up to 100 m or more can be recorded.

The energy threshold represents a crucial issue for the technique:
measurements are performed against the night sky background, and therefore the threshold is limited by the fluctuations of such background. As an example, that can be adapted to different configurations (as introduced in the previous section), the energy threshold is determined by the relation (computed for the number of photoelectrons):
$\frac{Signal}{\sqrt{Night-sky-bkg}} = \frac{N_{EAS-ph} \cdot A \cdot \varepsilon}{\sqrt{B \cdot A \cdot \varepsilon \cdot \tau \cdot \Omega}} = N_{EAS-ph} \sqrt{\frac{A \cdot \varepsilon}{B \cdot \tau \cdot \Omega}} > k$, where A=surface of light collector $\approx$ 100 $m^2$; $\varepsilon$ = quantum efficiency of the PMT photocatode $\approx$ 0.2; $\Omega$ = opening field of view $\approx 10^{-3}$ sr for a $1^o$ acceptance angle; $\tau$ = integration time (signal duration) $\approx$ 10 ns; B = night sky background $\approx 10^{12}$ ph/($m^2$ s sr); $N_{EAS-ph}$ = Number of photons from the shower $\approx$ 50 ph/$m^2$TeV (inside about 100 m from the shower axis). For a k value of 10, we obtain indicatively as energy threshold about 200 GeV (and in fact the energy thresholds of the present detectors are around 50-100 GeV [47, 48, 49]), with an acceptance area of the order of $3 \cdot 10^4$ $m^2$.

Of course, while space detectors can operate surrounded by an anticoincidence to identify the charged cosmic ray background, this cannot be performed in ground based observations. The main achievement of the new generation of detectors consists therefore in the possibility of distinguishing primary photons pointing to a specific direction, from the shape and orientation of the Cherenkov image obtained by means of cameras with pixels fields of view of the order of $0.1^o$. The performances have been additionally improved by stereoscopic observations[49]; the obtained energy and angular resolutions

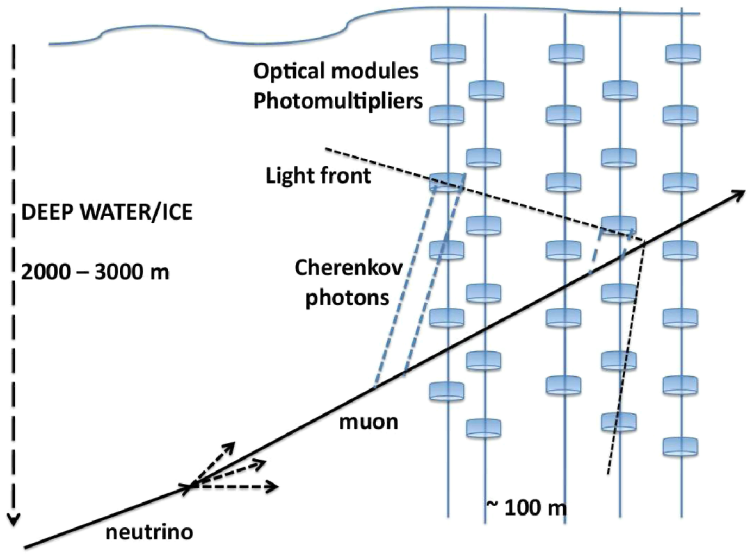


**FIGURE 8.** Scheme of underwater-underice high energy neutrino detectors. The up-going direction, and large depth, guarantees against the atmospheric muon background.

are respectively about 15% and 0.1°.

## HIGH ENERGY NEUTRINOS

To characterize the properties of neutrino detectors we have to focus on the neutrino cross section, i.e. approximately:
$\sigma(\nu_\mu) \approx 6.7 \cdot 10^{-36} \cdot E/TeV\ cm^2/n$, that for 1 km depth of water leads to an interaction probability of $P \approx 4 \cdot 10^{-7} \cdot E/TeV$ (above TeV energies, the dependence of cross section becomes $\sigma \propto E^{0.4}$ ). This implies very low signal rates, and therefore the requirement of very large detector volumes, adequately shielded against the background from the charged cosmic rays (i.e. deep underground or underwater). As relevant detection channel[12] we remind: $\nu_\mu + N \text{->} N + X + \mu$, where the detection can point to the hadron/e.m. cascade (from the "X" channel) and the througoing muon (the track-length of a TeV muon being about 2 km in water).

Therefore the detector sensitivity extends to a much wider volume than the physical dimension of the array. The muon-neutrino angle is $\theta_{\nu\mu} \approx 1.5^o/\sqrt{E_\nu/TeV}$ and therefore the direction can be reconstructed, following the reconstruction accuracy of the muon direction. The sea or ocean water (as well as deep ice) can provide at the same time the shielding material (see Fig. 8), the target, and the medium for producing the

[12] We cannot enter here into the discussion of the different channels, and the different neutrino species, that due to oscillations are present in nearly equal abundances among the primaries, but just get the general properties of the required installations.

Cherenkov light that can be detected by arrays of photomultipliers. A crucial property of the site has therefore to be the transparency of the medium (water,ice) in the Cherenkov light-photocathode sensitive spectral region (visible- blue). Typical best values of such transparency are of the order of 50 m for the attenuation length.

The number of photons/meter produced by a ultra-relativistic particle in water is about 400 photons/cm at an angle of $42^o$. In such conditions, with a PMT with photocathode area of 0.1 $m^2$, and quantum efficiency of 20%, taking into account the 50 m attenuation length of the light, the distance at which we obtain at least 1 photoelectron is of the order of 50-100 m. This should therefore be the scale of the array, indicating the density of sensitive elements.

Moreover, since the operation has to be at the photoelectron level, no other sources of light should add additional background (e.g. radioactivity and bioluminescence should be as low as possible). Progenitor of such projects was the DUMAND[50] program; such arrays have now been deployed or are under development in different sites: in lake water[51], antarctic ice[52], and mediterranean sea[53, 54, 55]. Neutrinos produced in the atmosphere by cosmic rays are currently detected. Detector dimensions of the order of the $km^3$ are evaluated to obtain physical results.

An appropriate shielding can as well be realized by exploiting the atmospheric depth at large zenith angles, provided that the detector has an high angular resolution. This opens the possibility of exploiting ground based arrays [56, 57], and therefore large installations as Auger[58], and in perspective the EAS radio emission (see next section).

## THE FUTURE: RADIO AND ACOUSTIC

In order to have a feeling about the future, we introduce here the detectors, now under development and that are expected to provide new information in the next few years.

- Radio emission from Extensive Air Sowers was first detected by Jelley et al (1965), and basic theory was developed. Electrons and positrons of the cascade emit synchrotron radiation in the Earth magnetic field. The emission frequency extends up to the GHz, but coherence (due to the spread of the shower particles) imposes for the optimum frequency region a limit around 100 MHz. The method was practically abandoned for years due to technical difficulties, mainly of energy calibration (and the problem of disentangling the interesting EAS signals from atmospheric disturbances). It was recently revitalized theoretically and experimentally by the LOPES Collaboration[59], operating on the KASCADE-Grande site (see also[60]). First LOPES results show:

a) The dependence of the signal on the shower angle to the Earth magnetic field, thus confirming a geomagnetic effect,

b) Good correlation with primary energy (represented by muon number measured by

KASCADE),

c) Good detection efficiency above $10^{17}$ eV. Tests and calibrations are going on, both at LOPES and at the Auger site.

- Radio signals correlated to e.m. cascades can have different origins. In particular, the positrons of the cascade can be annihilated by the electrons of the medium. This generates an excess of electrons in the cascade of about 20%, that behaves as a relativistic moving charge, therefore emitting Cherenkov radiation. The "charge" has the dimensions of the shower disc, and therefore the emission is coherent up to a maximum frequency (about GHz for a sufficiently dense material as ice, that is transparent to such radiation). The technique is suitable for realizing the huge acceptances required for UHE neutrino studies. The possibility of exploiting such effect for the detection of high energy cascades was pointed out by Askaryan in 1961[61]. The effect has been recently observed in laboratory[62], a detector has been calibrated[63], and first results have been reported[64].

- The energy loss by the cascade heats the medium, and therefore a pressure wave is generated. If the cascade dimensions are of the order of centimeters, as in water/ice, for energy releases above $10^{15}$ eV, the pressure wave can be detected with the present techniques[65]. Typical frequencies are of the order of 10 kHz, and therefore the technique can be interesting since the attenuation length in water is of the order of the km (much larger than the typical 50 m of visible Cherenkov light). The acoustic emission has been detected at accelerators[66, 67], the response is linear with energy, and test on the field (lake Baikal) are going on. The technique can first be associated to the quoted large scale optical installations.

## ACKNOWLEDGMENTS

Thanks to the organizers for their great efforts, to the students for their attention and patience, and to Oscar Saavedra for many useful advices. Ms. Altamirano would like to thank the Centro de Tecnologías de Información y Comunicaciones, Lima, Peru, for their support in undertaking this work.

## REFERENCES

1. M.S. Longair, *High Energy Astrophysics*, Cambridge University Press (1992)
2. P. Blasi, *High Energy Astrophysics*, Third School on Cosmic Rays and Astrophysics, 2008
3. J. Chirinos, *Introduction to Cosmic Rays*, Third School on Cosmic Rays and Astrophysics, 2008
4. B. Rossi, *Cosmic Rays*, McGraw-Hill (1964), *High Energy Particles*, Prentice-Hall, Inc. (1952)
5. L. Leprince-Ringuet, *Les Rayons Cosmiques*, Albin Michel Paris (1945)
6. O. Saavedra, *History of Cosmic Rays*, Third School on Cosmic Rays and Astrophysics, 2008
7. W.R. Leo, *Techniques for Nuclear and Particle Physics Experiments*, Springer, Berlin (1994)
8. J. Bellido, *Introduction to Detectors for Cosmic Rays*, Third School on Cosmic Rays and Astrophysics, 2008

9. McMurdo, http://www.spacedaily.com/news/uav-05k.html
10. HEAO-3 http://heasarc.gsfc.nasa.gov/docs/heao3/heao3.html; M. Bouffard et al, *Astrophysics and Space Science*, 84 (1982) 3
11. Review of Particle Physics, *Physics Letters B*, 592 (2004)
12. CRIS, http://www.srl.caltech.edu/ACE/CRIS_SIS/cris.html
13. PAMELA, http://pamela.roma2.infn.it/index.php
14. AMS, http://ams.cern.ch/AMS/Description/overview.html
15. S. Coutou, *Direct Measurements of Cosmic Rays*, Third School on Cosmic Rays and Astrophysics, 2008
16. http://astrophysics.gsfc.nasa.gov/astroparticles/programs/
17. K. Pretzl, *J. Phys. G: Nucl. Part. Phys.*, 31 (2005) R133
18. U. Amaldi, *Physica Scripta*, 23 (1981) 409.
19. N.L. Grigorov et al, *Sov. Jou. Nucl. Phys.*, 11/5 (1970) 588
20. C. Castagnoli et al, Nuovo Cim., 10 (1953) 1539
21. JACEE, http://marge.phys.washington.edu/jacee/
22. RUNJOB, http://runjob.boom.ru/
23. ATIC, http://www.atic.umd.edu/atic.html
24. CREAM, http://cosmicray.umd.edu/cream/
25. CGRO, http://heasarc.gsfc.nasa.gov/docs/cgro/cgro/
26. AGILE, http://agile.rm.iasf.cnr.it/.
27. GLAST, http://www.nasa.gov/glast
28. G. Cocconi, *Handbuch der Physik*, Springer-Verlag, 46/1 (1961) 215
29. G.V. Kulikov and G.B. Khristiansen, J.E.P.T., 35 (8) (1959) 441
30. EAS-TOP, http://www.lngs.infn.it/,
31. H. Hayashi et al, Nucl.Instr.Meth., A, 545 (2005) 643
32. KASCADE, KASCADE-Grande, http://www-ik.fzk.de/KASCADE_home.html
33. IceTop, http://icecube.bartol.udel.edu/
34. J. Linsley, *Phys. Rev. Lett.*, 10 (1963) 146
35. M.A. Lawrence et al, J.Phys.G, 17 (1991) 733
36. AGASA, http://www-akeno.icrr.u-tokyo.ac.jp/AGASA/
37. Pierre Auger Collaboration, http://www.auger.org/
38. CORSIKA, http://www-ik.fzk.de/corsika/
39. J. Knapp, *Air Shower Simulations*, Third School on Cosmic Rays and Astrophysics, 2008
40. R. Mussa, *Atmospheric Monitoring*, Third School on Cosmic Rays and Astrophysics, 2008
41. Tunka, http://dbserv.sinp.msu.ru/tunka/
42. D. Bird et al, *Astrophys. J.*, 441 (1995) 144
43. HiRes, http://www.cosmic-ray.org/
44. CASA-MIA Coll., *Phys. Rev. Lett.*, 79 (1997) 1805
45. Milagro, http://umdgrb.umd.edu/cosmic/milagro.html
46. Argo, http://argo.na.infn.it/
47. MAGIC, http://wwwmagic.mppmu.mpg.de/
48. VERITAS, http://veritas.sao.arizona.edu/
49. H.E.S.S., http://www.mpi-hd.mpg.de/hfm/HESS/HESS.shtml
50. DUMAND, http://www.phys.hawaii.edu/~dumand
51. BAIKAL, http://baikalweb.jinr.ru/
52. ICECUBE, http://www.icecube.wisc.edu/info/
53. ANTARES, http://antares.in2p3.fr/
54. NESTOR, http://www.nestor.noa.gr/
55. NEMO, http://nemoweb.lns.infn.it/
56. V.S. Berezinsky et al, *Astrophys. Space Sci.*, 32 (1975) 461
57. The EAS-TOP Coll., *Nucl. Phys. B*, 70 (1999) 509
58. Pierre Auger Coll., *Phys. Rev. Lett.*, 100 (2008) 211101
59. LOPES, http://www.astro.ru.nl/lopes/
60. CODALEMA, http://codalema.in2p3.fr/
61. G.A. Askaryan, *JETP*, 14 (1962) 441; 21 (1965) 658
62. D. Saltzberg et al, *Phys. Rev. Lett.*, 86 (2001) 2802

63. P.W. Gorham et al, *Phys. Rev. Lett.*, 99 (2007) 171101
64. ANITA, `http://amanda.uci.edu/~anita/`
65. G.A. Askaryan, *Atomic Energy*, 3 (1957) 152
66. L. Sulak et al, *Nucl. Instr. and Meth.*, 161 (1979) 203
67. V.I. Albul et al, *Instr. Exp. Tech.*, 44 (2001) 327